N-Substituted Guanidinate Anions as Ancillary Ligands in Group 4 Chemistry. Syntheses and Characterization of $M\{RNC[N(SiMe_3)_2]NR\}_2Cl_2$, $[M\{CyNC[N(SiMe_3)_2]NCy\}Cl_3]^-$ (M = Zr, Hf; R = ^{i}Pr, Cy), and $Zr\{CyNC[N(SiMe_3)_2]NCy\}(CH_2Ph)_3$

Dayna Wood, Glenn P. A. Yap, and Darrin S. Richeson*

Department of Chemistry, University of Ottawa, Ottawa, Ontario, Canada K1N 6N5

Received June 9, 1999

Addition of $N(SiMe_3)_2$ anion equivalents to carbodiimides, RN═C═NR (R = cyclohexyl, isopropyl), generated tetrasubstituted guanidinates which provided entry to a series of bis- and mono(guanidinate) complexes of Zr and Hf exhibiting the general formulas $\{RNC[N(SiMe_3)_2]NR\}_2MCl_2$ (R = isopropyl, M = Zr (**1**), Hf (**2**); R = cyclohexyl, M = Zr (**3**), Hf (**4**) and $\{CyNC[N(SiMe_3)_2]NCy\}MCl_4]^-$ (M = Zr (**5**), Hf (**6**)) depending on the metal:ligand ratio used in the reaction. In addition to spectroscopic characterization, definitive evidence for the molecular structures of these products is provided through single-crystal X-ray analyses for **1**, **3**, **4**, **5**, and **6**, which are presented. These results further define the ligand-bonding parameters and provide clear evidence that the planar $N(SiMe_3)_2$ functional groups and the MNCN planes have a nearly perpendicular orientation and therefore do not experience significant π overlap. Complex **5** provides an access to the organometallic derivative $\{CyNC[N(SiMe_3)_2]NCy\}Zr(CH_2Ph)_3$ (**7**) by reaction with 3 equiv of $PhCH_2MgCl$. Single-crystal X-ray analysis confirmed the connectivity of this species and indicated an η^2-benzyl group. These results provide the first reported example of an organozirconium complex supported by a guanidinate ligand.

Introduction

The search for alternatives to cyclopentadienyl-based ligands in early transition metal chemistry has generated a great deal of recent effort on preparing complexes with N-centered donor ligands.[1−14] In this regard we were attracted to N-substituted guanidinate anions, $[RNC(NR'_2)NR'']^-$, as potential bulky supporting ligands for group 4 metals. These ligands fall into a family of bidentate, three-atom bridging ligands with the general formula $RNXNR^-$ (X = CNR'_2,[15] CR′,[16,17] or N[18]). Substituted guanidinate ligands (X = CNR'_2, R′ ≠ H) (Scheme 1) present an interesting system for exploring the effects of making rational modifications to both the steric bulk and electronic properties of the supporting ligands through changes in the organic substituents on the nitrogen atoms. A key feature of guanidinate ligands is the presence of the NR'_2 function, which allows consideration of a zwitterionic resonance structure (**I**). Of course, for this contribution to be significant the NR'_2 center must be planar, sp^2 hybridized with the lone pair residing in a p orbital which would be available for overlap with the conjugated NCN moiety, and there must be a small dihedral angle between the planes defined by the CNR'_2 groups and that defined by NCN in order for substantial overlap to occur. Keeping in mind these two requirements, it is interesting to note that the attendant steric congestion caused by the two organic substituents would probably encourage a larger dihedral angle, thus discouraging the appropriate orientation for π conjugation.

Scheme 1

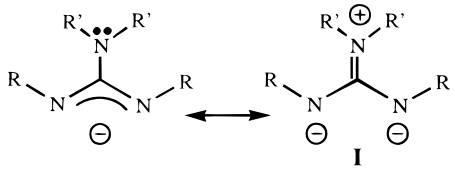

I

We wish to report a portion of our ongoing investigation into the incorporation of guanidinates and related ligands into metal complexes.[19−27] Included in this report are the syntheses and

(1) Togni, A.; Venanzi, L. M. *Angew. Chem., Int. Ed. Engl.* **1994**, *33*, 497.
(2) Brand, H.; Arnold, J. A. *Coord. Chem. Rev.* **1995**, *140*, 137.
(3) Stephan, D. W.; Guérin, F.; Spence, R. E. v. H.; Koch, L.; Gao, X.; Brown, S. J.; Swabey, J. W.; Wang, Q.; Xu, W.; Zoricak, P.; Harrison, D. G. *Organometallics* **1999**, *18*, 2046.
(4) Baumann, R.; Davis, W. M.; Schrock, R. R. *J. Am. Chem. Soc.* **1997**, *119*, 3830.
(5) Warren, T. H.; Schrock, R. R.; Davis, W. M. *Organometallics* **1998**, *17*, 308.
(6) Gibson, V. C.; Kimberley, B. S.; White, A. J. P.; Williams, D. J.; Howard, P. *J. Chem. Soc., Chem. Commun.* **1998**, 313.
(7) Schaller, C. P.; Cummins, C. C.; Wolczanski, P. T. *J. Am. Chem. Soc.* **1996**, *118*, 591.
(8) Schrock, R. R.; Cummins, C. C.; Wilhelm, T.; Lin, S.; Reid, S. M.; Kol, M.; Davis, W. M. *Organometallics* **1996**, *15*, 1470.
(9) Scollard, J. D.; McConville, D. H. *J. Am. Chem. Soc.* **1996**, *118*, 10008.
(10) Guérin, F.; McConville, D. H.; Vittal, J. J.; Yap, G. P. A. *Organometallics* **1998**, *17*, 5172 and references therein.
(11) Shapiro, P. J.; Cotter, W. D.; Schaefer, W. P.; Labinger, J. A.; Bercaw, J. E. *J. Am. Chem. Soc.* **1994**, *116*, 4623.
(12) Black, D. G.; Jordan, R. F.; Rogers, R. D. *Inorg. Chem.* **1997**, *36*, 103.
(13) Uhrhammer, R.; Black, D. G.; Gardner, T. G.; Olsen, J. D.; Jordan, R. F. *J. Am. Chem. Soc.* **1993**, *115*, 8493
(14) Jacoby, D.; Isoz, S.; Floriani, C.; Chiesi-Villa, A.; Rizzoli, C. *J. Am. Chem. Soc.* **1995**, *117*, 5801
(15) Mehrotra, R. C. In *Comprehensive Coordination Chemistry*; Wilkinson, G., Gillard, R. D., McCleverty, J. A., Eds.; Pergamon Press: Oxford, U.K., 1987; Chapter 13.8.
(16) Kilner, M.; Baker, J. *Coord. Chem. Rev.* **1994**, *133*, 219.
(17) Edelmann, F. T. *Coord. Chem. Rev.* **1994**, *137*, 403.
(18) Moore, D. S.; Robinson, S. D. *Adv. Inorg. Chem. Radiochem.* **1986**, *30*, 1.
(19) Tin, M. K. T.; Yap, G. P. A.; Richeson, D. S. *Inorg. Chem.* **1999**, *38*, 998.
(20) Tin, M. K. T.; Yap, G. P. A.; Richeson, D. S. *Inorg. Chem.* **1998**, *37*, 6728.

10.1021/ic990668i CCC: $18.00
Published on Web 11/24/1999

Scheme 2

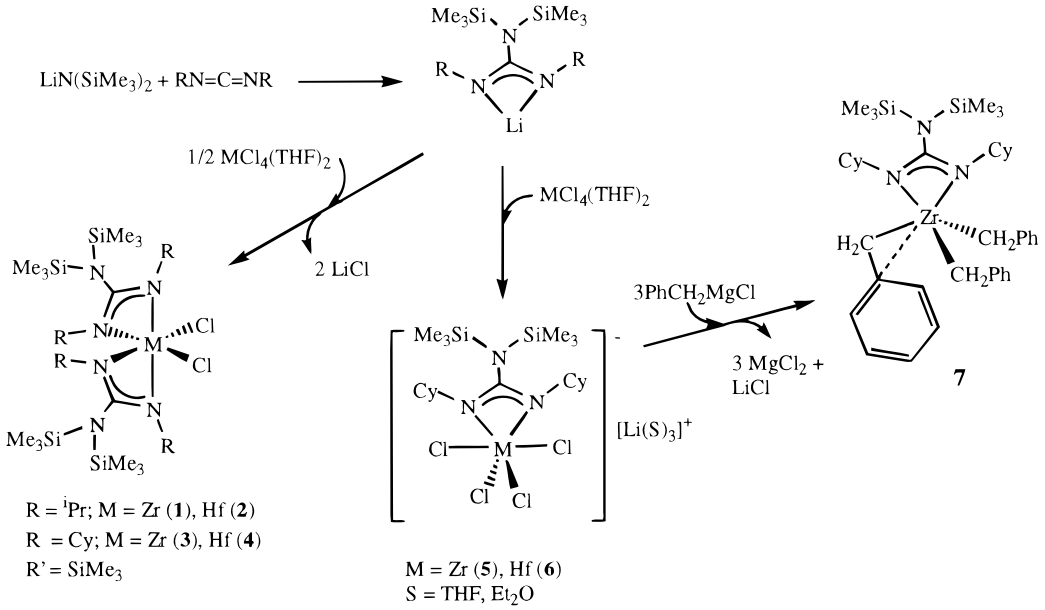

characterization of a novel family of bis(guanidinate) group 4 compounds of the general formula $M(RNC[N(SiMe_3)_2]NR)_2Cl_2$ (R = isopropyl, M = Zr (**1**), Hf (**2**); R = cyclohexyl, M = Zr (**3**), Hf (**4**)) and two mono(guanidinate) anionic complexes of formula $\{M(CyNC[N(SiMe_3)_2]NCy)Cl_3\}^-$ (M = Zr (**5**), Hf (**6**); Cy = cyclohexyl). Complex **5** is readily converted into the organometallic derivative $Zr\{CyNC[N(SiMe_3)_2]NCy\}(CH_2Ph)_3$ (**7**) by reaction with $C_6H_5CH_2MgCl$.

Results and Discussion

Bis(guanidinate) Complexes of Zr and Hf. Guanidinate anions were generated by the direct reaction of either 1,3-dicyclohexylcarbodiimide or 1,3-diisopropylcarbodiimide (RN=C=NR; R = Cy, iPr) with 1 equiv of $LiN(SiMe_3)_2$ in diethyl ether. The lithium salts could be isolated in pure form by simple removal of the solvent. However, in most cases metathesis reactions with Zr and Hf halides can be carried out with freshly prepared solutions of lithium guanidinate. For example, addition of 0.5 equiv of $MCl_4(THF)_2$ (M = Zr, Hf) to a solution of in situ prepared guanidinate followed by recrystallization resulted in isolation of the bis(guanidinate) complexes $M\{RNC[N(SiMe_3)_2]NR\}_2Cl_2$ (**1**−**4**) (Scheme 2). Spectroscopic characterization provided the first confirmation of the identity of these materials. Specifically, the four compounds exhibited similar ^1H and ^{13}C NMR spectra with the most notable features being (1) the appearance of single isopropyl or cyclohexyl substituents as indicated by single proton and carbon resonances for the NCH groups and (2) the appearance of one resonance for the $Si(CH_3)_3$ moieties of the NR'_2 groups. On the basis of the NMR observations and the results of the crystallographic characterization described below for **1** and **4**, we propose the C_2 symmetric structures for these complexes shown in Scheme 2. The fact that the two ends of the guanidinate ligand appear to be equivalent on the NMR time scale is consistent with compounds **1**−**4** being fluxional. We have previously observed this feature in analogous amidinate complexes of Zr, Hf, and Sn.[22−27] We have also previously noted that the incorporation of sterically more demanding substituents on the amidinate methyne carbon (e.g. tBu vs Me) can slow this fluxionality.[23, 27]

Table 1. Crystallographic Data for $\{iPrNC[N(SiMe_3)_2]NiPr\}_2ZrCl_2$ (**1**), $\{CyNC[N(SiMe_3)_2]NCy\}_2ZrCl_2$ (**3**), and $\{CyNC[N(SiMe_3)_2]NCy\}_2HfCl_2$ (**4**)

	1	**3**·toluene	**4**·0.5(benzene)
empirical formula	$C_{26}H_{64}Cl_2N_6Si_4Zr$	$C_{38}H_{80}Cl_2N_6Si_4Zr$	$C_{38}H_{80}Cl_2HfN_6Si_4$
fw	735.31	987.69	1018.76
temp (K)	203(2)	203(2)	213(2)
λ (Å)	0.710 73	0.710 73	0.710 73
space group	*Pbcn*	$P2_1/c$	$P2_1/c$
a (Å)	12.5453(17)	13.818(3)	13.7878(6)
b (Å)	17.701(2)	18.534(4)	18.5571(9)
c (Å)	18.012(2)	21.369(4)	21.4427(10)
β (deg)		92.716(4)	92.8210(10)
V (Å^3)	3999.9(9)	5466(2)	5479.7(4)
Z	4	4	4
d_{calcd} (g/cm^3)	1.221	1.200	1.235
abs coeff (mm^{-1})	0.552	0.421	2.119
R1[a]	0.0654	0.0428	0.0427
wR2[b]	0.1686	0.0755	0.1284

[a] $R1 = \sum||F_o| - |F_c||/\sum|F_o|$. [b] $wR2 = [\sum w(|F_o| - |F_c|)^2/\sum w|F_o|^2]^{1/2}$.

Single-crystal X-ray diffraction analyses of **1**, **3**, and **4** were undertaken in order to establish the coordination geometry of the metal center and the connectivity of the ligand for these compounds (Table 1). The results of these structural studies are displayed in Figures 1−3 and summarized in Tables 2−4. In all three cases, the metal center is in a distorted pseudooctahedral environment consisting of the four nitrogen atoms of two bidentate guanidinate anions with cis chloride ligands completing the coordination sphere. Table 2 presents a summary of selected bond distances and angles for **1**. This complex possesses a crystallographic C_2 axis bisecting the Cl−Zr−ClA axis which makes the two guanidinate ligands equivalent. The two nitrogens (N(1), N(2)) and bridging carbon atom (C(7)) for the guanidinate lie in a plane which includes the Zr atom. The termini of the

(21) Zhou, Y.; Yap, G. P. A.; Richeson, D. S. *Organometallics* **1998**, *17*, 4387.
(22) Foley, S. R.; Bensimon, C.; Richeson, D. S. *J. Am. Chem. Soc.* **1997**, *119*, 10359.
(23) Zhou, Y.; Richeson, D. S. *Inorg. Chem.* **1997**, *36*, 501.
(24) Zhou, Y.; Richeson, D. S. *J. Am. Chem. Soc.* **1996**, *118*, 10850.
(25) Zhou, Y.; Richeson, D. S. *Inorg. Chem.* **1996**, *35*, 2448.
(26) Zhou, Y.; Richeson, D. S. *Inorg. Chem.* **1996**, *35*, 1423.
(27) Littke, A.; Sleiman, N.; Bensimon, C.; Yap, G.; Brown, S.; Richeson, D. *Organometallics* **1998**, *17*, 446.

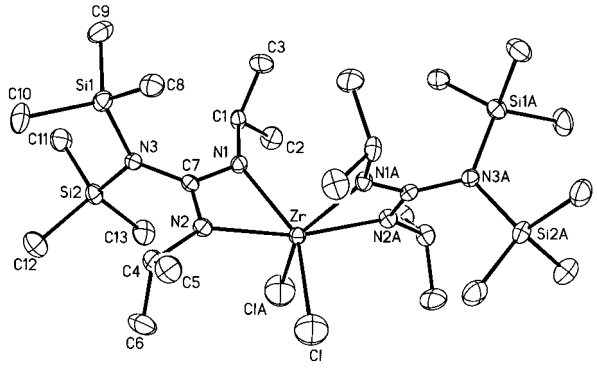

Figure 1. ORTEP diagram for (^{i}PrNC[N(SiMe$_3$)$_2$]N^{i}Pr)$_2$ZrCl$_2$ (**1**). Thermal ellipsoids are drawn at 30% probability. Hydrogen atoms have been omitted for clarity.

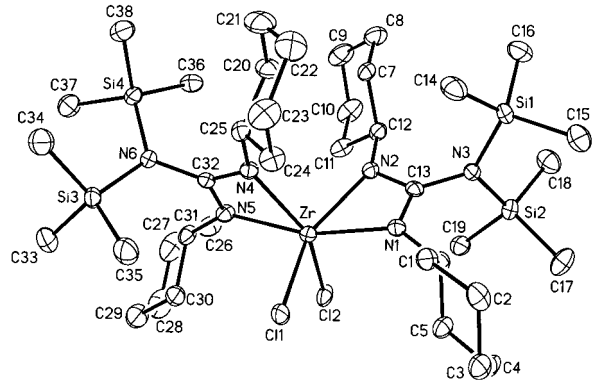

Figure 2. ORTEP diagram for (CyNC[N(SiMe$_3$)$_2$]NCy)$_2$ZrCl$_2$ (**3**). Thermal ellipsoids are drawn at 30% probability. Hydrogen atoms and solvent of crystallization (toluene) have been omitted for clarity.

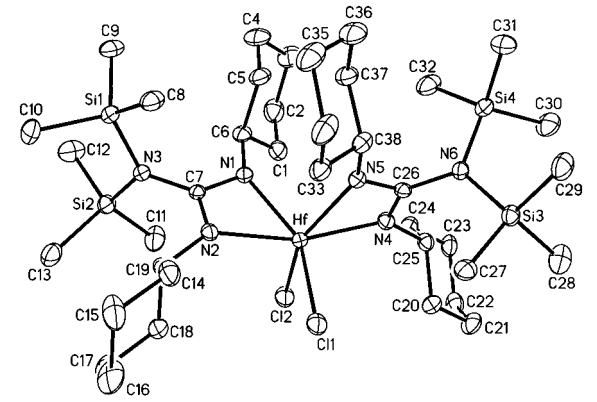

Figure 3. ORTEP diagram for (CyNC[N(SiMe$_3$)$_2$]NCy)$_2$HfCl$_2$ (**4**). Thermal ellipsoids are drawn at 30% probability. The solvent of crystallization (benzene) and hydrogen atoms have been omitted for clarity.

guanidinate ligand can be divided into two types, the cis N^{i}Pr groups (N(1), N(1)A) with a N−Zr−N angle of 98.1(2)° and trans N^{i}Pr groups (N(2), N(2)A) with a N−Zr−N angle of 164.9(2)°. The structural features of **1** are quite similar to those of the amidinate complex [CyNC(Me)NCy]$_2$ZrCl$_2$, which we recently reported.[27] Of particular interest in analyzing the steric requirements of these ligands is a comparison of the angles around the N atoms in **1** and in [CyNC(Me)NCy]$_2$ZrCl$_2$ (Chart 1). It is noteworthy that the C(bridge)−N−R (R = Cy, ^{i}Pr) angle and the Zr−N−R angle for these two species are comparable, indicating that although the substituent on the methyne carbon is larger in **1** (N(SiMe$_3$)$_2$ vs Me), the effective steric effects within the ligand framework are nearly the same.

Table 2. Selected Bond Lengths (Å) and Angles (deg) for {^{i}PrNC[N(SiMe$_3$)$_2$]N^{i}Pr}$_2$ZrCl$_2$ (**1**)

Distances			
Zr−N(1)	2.219(4)	N(2)−C(7)	1.343(6)
Zr−N(2)	2.264(4)	N(2)−C(4)	1.480(6)
Zr−Cl	2.420(2)	N(3)−C(7)	1.408(6)
Zr−C(7)	2.700(5)	C(1)−C(2)	1.504(7)
Si(1)−N(3)	1.770(4)	C(1)−C(3)	1.526(8)
Si(2)−N(3)	1.775(4)	C(4)−C(5)	1.494(7)
N(1)−C(7)	1.345(6)	C(4)−C(6)	1.534(8)
N(1)−C(1)	1.462(6)		
Angles			
N(1)A−Zr−N(1)	98.1(2)	ClA−Zr−C(7)	96.13(11)
N(1)A−Zr−N(2)	109.91(14)	C(7)A−Zr−C(7)	131.6(2)
N(1)−Zr−N(2)	59.15(14)	C(7)−N(1)−C(1)	123.0(4)
N(2)A−Zr−N(2)	164.9(2)	C(7)−N(1)−Zr	95.4(3)
N(1)A−Zr−Cl	94.49(12)	C(1)−N(1)−Zr	140.5(3)
N(1)−Zr−Cl	147.82(12)	C(7)−N(2)−C(4)	121.9(4)
N(2)A−Zr−Cl	101.99(12)	C(7)−N(2)−Zr	93.4(3)
N(2)−Zr−Cl	88.73(11)	C(4)−N(2)−Zr	142.7(3)
Cl−Zr−ClA	90.23(12)	C(7)−N(3)−Si(1)	118.8(3)
N(1)A−Zr−C(7)A	29.72(14)	C(7)−N(3)−Si(2)	119.6(3)
N(1)−Zr−C(7)A	109.37(15)	Si(1)−N(3)−Si(2)	121.6(2)
N(2)A−Zr−C(7)A	29.77(13)	N(1)−C(1)−C(2)	109.4(4)
N(2)−Zr−C(7)A	139.49(15)	N(1)−C(1)−C(3)	110.4(4)
Cl−Zr−C(7)A	96.13(11)	C(2)−C(1)−C(3)	110.3(5)
ClA−Zr−C(7)A	118.13(12)	N(2)−C(4)−C(5)	111.1(4)
N(1)A−Zr−C(7)	109.37(14)	N(2)−C(4)−C(6)	110.6(4)
N(1)−Zr−C(7)	29.72(14)	C(5)−C(4)−C(6)	109.8(5)
N(2)A−Zr−C(7)	139.49(15)	N(2)−C(7)−N(1)	110.8(4)
N(2)−Zr−C(7)	29.77(13)	N(2)−C(7)−N(3)	125.2(4)
Cl−Zr−C(7)	118.13(12)	N(1)−C(7)−N(3)	124.0(4)

Chart 1

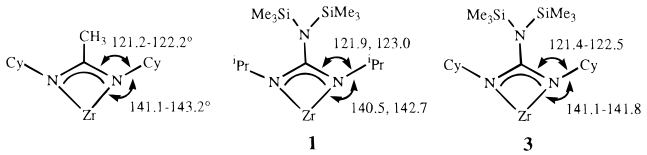

An alternative description of the Zr coordination geometry of **1** is as a distorted pseudotetrahedral complex with the vectors that bisect the guanidinate ligands, Zr−C(7) and Zr−C(7)A defining two of the vertexes and the two Zr−Cl vectors defining the other two. This description emphasizes the relationship of **1**−**4** to metallocene dichloride systems and allows some comparison of the structural features between these species. For example the C(7)−Zr−C(7)A angle in **1** of 131.6(2)° is very similar to the Cp(centroid)−Zr−Cp(centroid) angle of 134° found in Cp$_2$ZrCl$_2$.[28] However, the Zr−Cl distance (2.420(2) Å) and Cl−Zr−Cl angle (90.23(12)°) in **1** are both smaller than the corresponding values found for Cp$_2$ZrCl$_2$ (2.44 Å and 97.1°).

Monomeric complexes **3** and **4** crystallize with the molecular geometries shown in Figures 2 and 3. These compounds exhibited geometric and structural features similar to those of **1**. In both cases, the metal centers lie on an approximate 2-fold axis which bisects the Cl(1)−M−Cl(2) angle (M = Zr = 94.06(3)°; M = Hf = 93.81(7)°) with two planar bidentate guanidinate anions. Tables 3 and 4 present a summary of selected bond distances and angles for complexes **3** and **4**, respectively. As with **1**, the termini of the planar guanidinate ligands in these complexes can be divided into cis NCy groups and trans NCy groups. Again, an alternative pseudotetrahedral description based on the Zr−Cl(1), Zr−Cl(2), Zr−C(13), and Zr−C(32) vectors in **3** and the Hf−Cl(1), Hf−Cl(2), Hf−C(7), and Hf−C(26) vectors in **4** also provides satisfactory descriptions.

(28) Prout, K.; Cameron, T. S.; Forder, R. A.; Critchley, S. R.; Denton, B.; Rees, G. V. *Acta Crystallogr.* **1974**, *B30*, 2290.

Table 3. Selected Bond Lengths (Å) and Angles (deg) for $\{CyNC[N(SiMe_3)_2]NCy\}_2ZrCl_2$ (**3**)

		Distances	
Zr−N(4)	2.1991(19)	N(1)−C(6)	1.471(3)
Zr−N(2)	2.213(2)	N(2)−C(13)	1.334(3)
Zr−N(1)	2.216(2)	N(2)−C(12)	1.462(3)
Zr−N(5)	2.232(2)	N(3)−C(13)	1.413(3)
Zr−Cl(1)	2.4229(8)	N(4)−C(32)	1.331(3)
Zr−Cl(2)	2.4259(8)	N(4)−C(25)	1.463(3)
Zr−C(13)	2.670(3)	N(5)−C(32)	1.348(3)
Zr−C(32)	2.672(3)	N(5)−C(31)	1.471(3)
N(1)−C(13)	1.335(3)	N(6)−C(32)	1.418(3)
		Angles	
N(4)−Zr−N(2)	94.91(7)	C(13)−N(1)−Zr	94.24(16)
N(4)−Zr−N(1)	108.25(7)	C(6)−N(1)−Zr	141.16(16)
N(2)−Zr−N(1)	59.46(7)	C(13)−N(2)−C(12)	122.5(2)
N(4)−Zr−N(5)	59.67(7)	C(13)−N(2)−Zr	94.37(15)
N(2)−Zr−N(5)	108.04(7)	C(12)−N(2)−Zr	141.79(17)
N(1)−Zr−N(5)	163.40(7)	C(13)−N(3)−Si(2)	118.60(16)
N(4)−Zr−Cl(1)	93.02(6)	C(13)−N(3)−Si(1)	119.33(15)
N(2)−Zr−Cl(1)	149.20(6)	Si(2)−N(3)−Si(1)	121.95(12)
N(1)−Zr−Cl(1)	89.80(5)	C(32)−N(4)−C(25)	122.1(2)
N(5)−Zr−Cl(1)	101.65(5)	C(32)−N(4)−Zr	95.20(15)
N(4)−Zr−Cl(2)	148.32(6)	C(25)−N(4)−Zr	141.71(16)
N(2)−Zr−Cl(2)	94.62(5)	C(32)−N(5)−C(31)	121.5(2)
N(1)−Zr−Cl(2)	102.61(5)	C(32)−N(5)−Zr	93.27(15)
N(5)−Zr−Cl(2)	88.66(5)	C(31)−N(5)−Zr	141.05(16)
Cl(1)−Zr−Cl(2)	94.06(3)	C(32)−N(6)−Si(4)	118.65(16)
N(4)−Zr−C(13)	106.46(7)	C(32)−N(6)−Si(3)	119.72(16)
N(2)−Zr−C(13)	29.89(7)	Si(4)−N(6)−Si(3)	121.63(12)
N(1)−Zr−C(13)	29.90(7)	N(2)−C(13)−N(1))	110.8(2
N(5)−Zr−C(13)	137.75(8)	N(2)−C(13)−N(3)	123.9(2)
Cl(1)−Zr−C(13)	119.60(6)	N(1)−C(13)−N(3)	125.3(2)
Cl(2)−Zr−C(13)	96.65(5)	N(2)−C(13)−Zr	55.74(12)
N(4)−Zr−C(32)	29.75(7)	N(1)−C(13)−Zr	55.86(13)
N(2)−Zr−C(32)	106.22(7)	N(3)−C(13)−Zr	170.32(16)
N(1)−Zr−C(32)	137.77(7)	N(4)−C(32)−N(5)	110.8(2)
N(5)−Zr−C(32)	30.23(7)	N(4)−C(32)−N(6)	124.8(2)
Cl(1)−Zr−C(32)	95.24(5)	N(5)−C(32)−N(6)	124.4(2)
Cl(2)−Zr−C(32)	118.72(6)	N(4)−C(32)−Zr	55.05(12)
C(13)−Zr−C(32)	128.62(7)	N(5)−C(32)−Zr	56.50(12)
C(13)−N(1)−C(6)	121.4(2)	N(6)−C(32)−Zr	170.91(16)

The dihedral angle formed by the planar $N(SiMe_3)_2$ function and the MNCN plane offers a means of evaluating the possibility of π overlap between these two moieties. In the case of **1**, an angle of 88.2(4)° is formed between these two planes, while for **3** and **4**, average dihedral angles of 86.3 and 85.8° were observed for the two crystallographically unique guanidinate ligands in each of these two complexes. This nearly perpendicular disposition is likely the result of steric interactions between the isopropyl or cyclohexyl functions and the bulky trimethylsilyl groups and eliminates significant π conjugation in both **1** and **4**. As a result, structure **I** does not appear to be a significant contributor in these cases. However, this orientation of the bulky $N(SiMe_3)_2$ group effectively adds a third dimension to the steric bulk of what would be an otherwise planar guanidinate ligand. This perpendicular orientation also explains the observation that the guanidinate ligand in **1** appears to exhibit bonding parameters similar to those of the amidinate anion in $[CyNC(Me)NCy]_2ZrCl_2$ (Chart 1).

Mono(guanidinate) Complexes. A single tetrasubstituted guanidinate ligand can be introduced into the metal coordination sphere through reaction of a 1:1 ratio of lithium salt of *N*,*N*′-dicylohexyl-*N*″-bis(trimethylsilyl)guanidinate with either Zr or Hf chlorides. After crystallization from diethyl ether or THF, the new "ate" complexes $\{CyNC[N(SiMe_3)_2]NCy\}MCl_4]Li(S)_x$ (Scheme 2) (S = THF or THF/Et_2O) were isolated. The first indication that solvated Li cations remained in these materials was the appearance of coordinated solvent peaks in the NMR spectra of **5** and **6**. These spectra also display the characteristic signals for the guanidinate ligand.

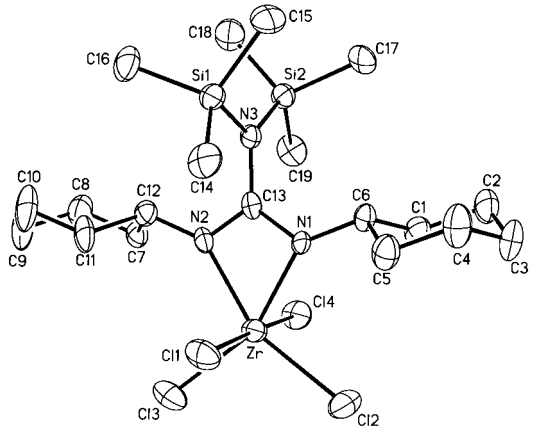

Figure 4. ORTEP diagram for $[\{CyNC[N(SiMe_3)_2]NCy\}ZrCl_4]^-$ (**5**). Thermal ellipsoids are drawn at 30% probability. The lithium cation with coordinated solvent molecules and hydrogen atoms have been omitted for clarity.

Table 4. Selected Bond Lengths (Å) and Angles (deg) for $\{CyNC[N(SiMe_3)_2]NCy\}_2HfCl_2$ (**4**)

		Distances	
Hf−N(1)	2.181(4)	N(1)−C(6)	1.465(7)
Hf−N(5)	2.202(5)	N(2)−C(7)	1.339(7)
Hf−N(4)	2.211(5)	N(2)−C(19)	1.468(7)
Hf−N(2)	2.215(5)	N(3)−C(7)	1.418(7)
Hf−Cl(2)	2.411(2)	N(4)−C(26)	1.344(7)
Hf−Cl(1)	2.414(2)	N(4)−C(25)	1.461(7)
Hf−C(7)	2.656(5)	N(5)−C(26)	1.338(7)
Hf−C(26	2.666(5)	N(5)−C(38)	1.461(7)
N(1)−C(7)	1.342(7)	N(6)−C(26)	1.404(7)
		Angles	
N(1)−Hf−N(5)	95.1(2)	Cl(2)−Hf−C(26)	120.42(12)
N(1)−Hf−N(4)	108.0(2)	Cl(1)−Hf−C(26)	95.80(12)
N(5)−Hf−N(4)	59.9(2)	C(7)−Hf−C(26)	128.8(2)
N(1)−Hf−N(2)	60.1(2)	C(7)−N(1)−C(6)	121.5(5)
N(5)−Hf−N(2)	107.7(2)	C(7)−N(1)−Hf	94.9(3)
N(4)−Hf−N(2)	163.5(2)	C(6)−N(1)−Hf	142.7(4)
N(1)−Hf−Cl(2)	92.54(13)	C(7)−N(2)−C(19)	121.8(5)
N(5)−Hf−Cl(2)	150.16(13)	C(7)−N(2)−Hf	93.4(3)
N(4)−Hf−Cl(2)	90.35(13)	C(19)−N(2)−Hf	140.5(4)
N(2)−Hf−Cl(2)	101.12(13)	C(7)−N(3)−Si(2)	120.1(4)
N(1)−Hf−Cl(1)	149.51(13)	C(7)−N(3)−Si(1)	118.8(4)
N(5)−Hf−Cl(1)	94.09(13)	Si(2)−N(3)−Si(1)	121.2(3)
N(4)−Hf−Cl(1)	101.78(14)	C(26)−N(4)−C(25)	121.3(5)
N(2)−Hf−Cl(1)	89.38(12)	C(26)−N(4)−Hf	94.0(3)
Cl(2)−Hf−Cl(1)	93.81(7)	C(25)−N(4)−Hf	141.2(4)
N(1)−Hf−C(7)	30.2(2)	C(26)−N(5)−C(38)	122.1(5)
N(5)−Hf−C(7)	106.2(2)	C(26)−N(5)−Hf	94.6(3)
N(4)−Hf−C(7)	138.0(2)	C(38)−N(5)−Hf	142.1(4)
N(2)−Hf−C(7)	30.2(2)	C(26)−N(6)−Si(3)	118.4(4)
Cl(2)−Hf−C(7)	94.69(12)	C(26)−N(6)−Si(4)	119.9(4)
Cl(1)−Hf−C(7)	119.41(12)	Si(3)−N(6)−Si(4)	121.6(3)
N(1)−Hf−C(26)	106.5(2)	N(2)−C(7)−N(1)	110.5(5)
N(5)−Hf−C(26)	30.0(2)	N(2)−C(7)−N(3)	124.7(5)
N(4)−Hf−C(26)	30.2(2)	N(1)−C(7)−N(3)	124.8(5)
N(2)−Hf−C(26)	137.5(2)		

The proposed structures for **5** and **6** (Scheme 2) were confirmed by X-ray crystallographic characterization, which yielded the results summarized in Figures 4 and 5 and Tables 5−7. In both cases, the complexes possessed a single bidentate guanidinate and four chloro ligands, giving a distorted octahedral coordination geometry. The guanidinate ligands occupy two of the octahedral sites and exhibit bonding parameters that are similar to each other and to those of the bis(guanidinate) complexes **1**, **3**, and **4**. The coordination geometry of these two

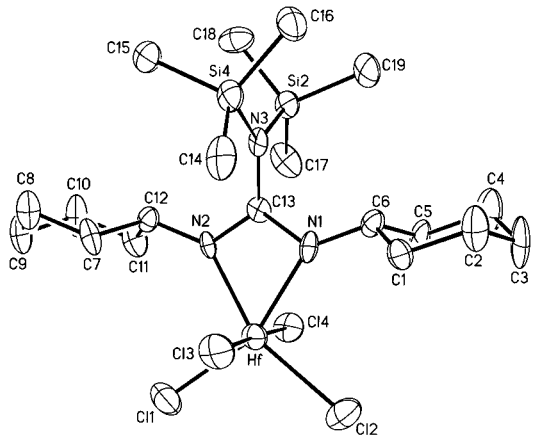

Figure 5. ORTEP diagram for $[\{CyNC[N(SiMe_3)_2]NCy\}HfCl_4]^-$ (**6**). Thermal ellipsoids are drawn at 30% probability. The lithium cation with coordinated solvent molecules and hydrogen atoms have been omitted for clarity.

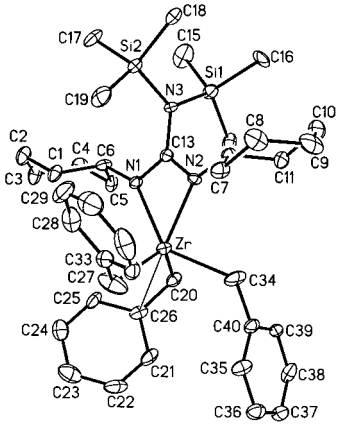

Figure 6. ORTEP diagram for $\{CyNC[N(SiMe_3)_2]NCy\}Zr(CH_2Ph)_3$ (**7**). Thermal ellipsoids are drawn at 30% probability. Hydrogen atoms have been omitted for clarity.

Table 5. Crystallographic Data for $\{CyNC[N(SiMe_3)_2]NCy\}ZrCl_4]Li(THF)_2(Et_2O)$ (**5**), $\{CyNC[N(SiMe_3)_2]NCy\}HfCl_4]Li(THF)_3$ (**6**), and $\{CyNC[N(SiMe_3)_2]NCy\}Zr(CH_2Ph)_3$ (**7**)

	5	**6**	**7**
empirical formula	$C_{31}H_{66}Cl_4LiN_3O_3Si_2Zr$	$C_{31}H_{64}Cl_4HfLiN_3O_3Si_2$	$C_{40}H_{61}N_3Si_2Zr$
fw	825.01	910.26	731.32
temp (K)	203(2)	223(2)	203(2)
λ (Å)	0.710 73	0.710 73	0.710 73
space group	*Pbcn*	*Pbcn*	$P2_1/n$
a (Å)	33.284(7)	33.460(2)	10.483(1)
b (Å)	14.956(3)	15.0033(8)	18.889(2)
c (Å)	17.381(4)	17.3857(9)	20.459(3)
β (deg)			102.431(2)
V (Å^3)	8652(3)	8727.8(8)	3956.0(9)
Z	8	8	4
d_{calcd} (g/cm^3)	1.267	1.385	1.228
abs coeff (mm^{-1})	0.588	2.721	0.369
R1[a]	0.0802	0.0937	0.0473
wR2[b]	0.2408	0.2385	0.0918

[a] $R1 = \sum||F_o| - |F_c||/\sum|F_o|$. [b] $wR2 = [\sum w(|F_o| - |F_c|)^2/\sum w|F_o|^2]^{1/2}$.

complexes can also be reasonably described as pseudotrigonal bipyramidal with the central C of the guanidinate ligand and cis chloro ligands forming the equatorial plane (C(13), Cl(2), and Cl(3) for **5** and C(13), Cl(1), and Cl(2) for **6**). The dihedral angles formed between the two planes defined by the $N(SiMe_3)_2$ function and the MNCN cycle again indicate little π-bonding interaction between these moieties (85.8(7)° for **5** and 86.0(9)° for **6**).

Table 6. Bond Lengths (Å) and Angles (deg) for $[\{CyNC[N(SiMe_3)_2]NCy\}ZrCl_4][Li(THF)_2(Et_2O)]$ (**5**)

Distances			
Zr−N(2)	2.179(7)	Si(2)−N(3)	1.768(6)
Zr−N(1)	2.181(6)	Si(2)−C(19)	1.852(9)
Zr−Cl(4)	2.423(2)	Si(2)−C(18)	1.849(10)
Zr−Cl(2)	2.434(3)	Si(2)−C(17)	1.862(9)
Zr−Cl(3)	2.441(3)	Cl(1)−Li	2.39(2)
Zr−Cl(1)	2.544(2)	N(1)−C(13)	1.312(10)
Zr−C(13)	2.641(9)	N(1)−C(6)	1.466(10)
Si(1)−N(3)	1.758(6)	N(2)−C(13)	1.336(10)
Si(1)−C(14)	1.855(9)	N(2)−C(12)	1.469(10)
Si(1)−C(16)	1.849(9)	N(3)−C(13)	1.426(11)
Si(1)−C(15)	1.889(9)		
Angles			
Si(1)−N(3)−Si(2)	124.0(4)	Cl(3)−Zr−C(13)	127.72(19)
N(1)−C(13)−N(2)	110.7(7)	Cl(1)−Zr−C(13)	89.07(15)
N(1)−C(13)−N(3)	125.3(7)	N(3)−Si(1)−C(14)	108.4(4)
N(2)−C(13)−N(3)	124.0(7)	N(3)−Si(1)−C(16)	113.5(4)
N(1)−C(13)−Zr	55.4(4)	C(13)−N(1)−C(6)	123.6(7)
N(2)−C(13)−Zr	55.4(4)	C(13)−N(1)−Zr	94.9(5)
N(3)−C(13)−Zr	177.7(5)	C(6)−N(1)−Zr	141.4(5)
N(2)−Zr−N(1)	60.0(2)	C(13)−N(2)−C(12)	123.7(7)
N(2)−Zr−Cl(4)	92.77(18)	C(13)−N(2)−Zr	94.3(5)
N(1)−Zr−Cl(4)	93.07(17)	C(12)−N(2)−Zr	141.9(5)
N(2)−Zr−Cl(2)	155.00(19)	C(13)−N(3)−Si(1)	118.0(5)
N(1)−Zr−Cl(2)	95.14(18)	C(13)−N(3)−Si(2)	117.9(5)
Cl(4)−Zr−Cl(2)	90.70(10)	C(13)−N(1)−C(6)	123.6(7)
N(2)−Zr−Cl(3)	97.49(18)	C(13)−N(1)−Zr	94.9(5)
N(1)−Zr−Cl(3)	157.15(18)	C(6)−N(1)−Zr	141.4(5)
Cl(4)−Zr−Cl(3)	91.63(9)	C(13)−N(2)−C(12)	123.7(7)
Cl(2)−Zr−Cl(3)	107.16(11)	C(13)−N(2)−Zr	94.3(5)
N(2)−Zr−Cl(1)	89.18(18)	C(12)−N(2)−Zr	141.9(5)
N(1)−Zr−Cl(1)	88.60(17)	C(13)−N(3)−Si(1)	118.0(5)
Cl(4)−Zr−Cl(1)	177.89(9)	C(13)−N(3)−Si(2)	117.9(5)
Cl(2)−Zr−Cl(1)	87.87(10)	C(13)−N(1)−C(6)	123.6(7)
Cl(3)−Zr−Cl(1)	87.32(9)	C(13)−N(1)−Zr	94.9(5)
N(2)−Zr−C(13)	30.3(2)	C(6)−N(1)−Zr	141.4(5)
N(1)−Zr−C(13)	29.7(2)	C(13)−N(2)−C(12)	123.7(7)
Cl(4)−Zr−C(13)	93.01(15)	C(13)−N(2)−Zr	94.3(5)
Cl(2)−Zr−C(13)	124.80(19)		

Charge compensation for these anionic complexes is provided in both cases by a Li cation which is associated with one of the chloro ligands (2.39(2) Å in **5** and 2.42(6) Å in **6**). Tetrahydrofuran or a combination of diethyl ether and THF completes the coordination spheres of the Li cations.

Preparation and Structural Characterization of $\{CyNC[N(SiMe_3)_2]NCy\}Zr(CH_2Ph)_3$ (7). The reaction of **5** with 3 equiv of $PhCH_2MgCl$ proceeded according to the metathesis reaction shown in Scheme 2 to yield complex **7**. Spectroscopic characterization indicated the incorporation of three benzyl groups and was consistent with the formulation of this species as $\{CyNC[N(SiMe_3)_2]NCy\}Zr(CH_2Ph)_3$. Both the ^{13}C and ^1H NMR spectra indicated a single Cy substituent and a single benzyl group and gave no evidence of an η^2-benzyl ligand.

The molecular structure of **7** was determined, and an ORTEP diagram is provided in Figure 6 and crystallographic data are summarized in Tables 5 and 8. The geometry of the five-coordinate Zr center is better described as distorted tetrahedral with vertexes defined by the three benzyl groups and the central carbon (C(13)) of the guanidinate ligand. The corresponding angles range from 118.2(3) to 90.7(2)° with an average value of 107.8°.

The average $Zr-CH_2$ bond distance is 2.273(6) Å, which is shorter than the corresponding distances in the recently reported

Table 7. Selected Bond Lengths (Å) and Angles (deg) for [{CyNC[N(SiMe$_3$)$_2$]NCy}HfCl$_4$][Li(THF)$_3$] (**6**)

Distances			
Hf−N(2)	2.17(2)	N(1)−C(13)	1.32(2)
Hf−N(1)	2.19(2)	N(1)−C(6)	1.42(2)
Hf−Cl(3)	2.402(6)	N(2)−C(13)	1.34(2)
Hf−Cl(1)	2.427(6)	N(2)−C(12)	1.46(2)
Hf−Cl(2)	2.424(6)	N(3)−C(13)	1.41(2)
Hf−Cl(4)	2.524(5)	N(3)−Si(2)	1.759(14)
Hf−C(13)	2.63(2)	N(3)−Si(4)	1.79(2)
		Cl(4)−Li	2.42(6)

Angles			
Cl(4)−Hf−C(13)	89.2(4)	N(1)−Hf−Cl(2)	97.8(5)
C(13)−N(1)−C(6)	124(2)	Cl(3)−Hf−Cl(2)	91.3(2)
C(13)−N(1)−Hf	94.0(12)	Cl(1)−Hf−Cl(2)	105.8(2)
C(6)−N(1)−Hf	141.5(14)	N(2)−Hf−Cl(4)	88.7(4)
C(13)−N(2)−C(12)	125(2)	N(1)−Hf−Cl(4)	89.4(4)
C(13)−N(2)−Hf	94.3(12)	Cl(3)−Hf−Cl(4)	177.9(2)
C(12)−N(2)−Hf	140.7(13)	Cl(1)−Hf−Cl(4)	87.7(2)
C(13)−N(3)−Si(2)	119.1(12)	Cl(2)−Hf−Cl(4)	87.3(2)
C(13)−N(3)−Si(4)	118.5(11)	N(2)−Hf−C(13)	30.6(6)
Si(2)−N(3)−Si(4)	122.3(10)	N(1)−Hf−C(13)	30.0(5)
N(1)−C(13)−N(2)	111(2)	Cl(3)−Hf−C(13)	92.9(4)
N(2)−Hf−N(1)	60.6(6)	Cl(1)−Hf−C(13)	126.1(5)
N(2)−Hf−Cl(3)	93.2(4)	Cl(2)−Hf−C(13)	127.7(5)
N(1)−Hf−Cl(3)	92.3(4)	N(1)−C(13)−N(3)	126(2)
N(2)−Hf−Cl(1)	95.6(4)	N(2)−C(13)−N(3)	123(2)
N(1)−Hf−Cl(1)	156.1(5)	N(1)−C(13)−Hf	56.0(10)
Cl(3)−Hf−Cl(1)	91.2(2)	N(2)−C(13)−Hf	55.1(10)
N(2)−Hf−Cl(2)	158.0(4)	N(3)−C(13)−Hf	177.0(13)

β-ketimino complex (TTP)Zr(CH$_2$Ph)$_3$ (TTP = 2-*p*-tolylamino-4-*p*-tolylimino-2-pentenato) which averaged 2.290(5) Å (Zr−C−C$_{ipso}$ = 99.1(2)°)[29] or that in CpZr(CH$_2$Ph)$_3$ at 2.299(8) Å (Zr−C$_{ispo}$ = 2.818(8) Å, Zr−C−C$_{ipso}$ = 94.5(5)°).[30]

One of the benzyl groups in **7** is unique in exhibiting a significantly more acute Zr−C−C$_{ipso}$ angle (Zr−C(20)−C(26) = 88.7(4)° vs Zr−C(27)−C(33) = 116.0(5)° and Zr−C(34)−C(40) = 123.2(4)°) and a short Zr−C$_{ipso}$ (Zr−C(26)) distance of 2.672(6) Å. These features establish that the phenyl group of this moiety is a weak electron donor and contrast with those of (TTP)Zr(CH$_2$Ph)$_3$ (Zr−C−C$_{ipso}$ = 99.1(2)°)[29] and CpZr(CH$_2$Ph)$_3$ at 2.299(8) Å (Zr−C$_{ispo}$ = 2.818(8) Å, Zr−C−C$_{ipso}$ = 94.5(5)°),[30] possibly indicating that the Zr center in **7** is more electron deficient than that in these complexes. Supporting this is the observation of similar bonding parameters observed in related tribenzyl complexes supported by bulky aryloxides in which the η^2-benzyl exhibited a Zr−C−C$_{ipso}$ angle of 84.3(9)° (Zr−CH$_2$ = 2.28 Å, Zr−C$_{ispo}$ = 2.59 Å)[31] and the structurally characterized cationic species [Cp$_2$Zr(CH$_2$Ph)NCCH$_3$]$^+$ (Zr−CH$_2$ = 2.344(8) Å, Zr−C$_{ispo}$ = 2.648(6) Å, Zr−C−C$_{ipso}$ = 84.9(4)°)[32,33] For reference, Zr(CH$_2$Ph)$_4$ exhibits a mean Zr−C−C$_{ipso}$ angle of 92(1)° (range from 85 to 101°).[34] Several other electron-deficient early transition metal complexes also exhibit similar features.[35−38]

Table 8. Selected Bond Lengths (Å) and Angles (deg) for {CyNC[N(SiMe$_3$)$_2$]NCy}Zr(CH$_2$Ph)$_3$ (**7**)

Distances			
Zr−N(1)	2.241(4)	N(1)−C(6)	1.465(6)
Zr−N(2)	2.250(5)	N(2)−C(13)	1.344(7)
Zr−C(27)	2.263(7)	N(2)−C(12)	1.461(6)
Zr−C(20)	2.268(5)	N(3)−C(13)	1.421(7)
Zr−C(34)	2.288(6)	C(20)−C(26)	1.466(8)
Zr−C(26)	2.672(6)	C(21)−C(26)	1.417(8)
Zr−C(13)	2.683(6)	C(25)−C(26)	1.385(8)
Si(1)−N(3)	1.756(5)	C(27)−C(33)	1.463(9)
Si(2)−N(3)	1.775(4)	C(34)−C(40)	1.491(8)
N(1)−C(13)	1.339(7)		

Angles			
N(1)−Zr−N(2)	59.77(17)	C(13)−N(1)−C(6)	122.7(5)
N(1)−Zr−C(27)	111.7(3)	C(13)−N(1)−Zr	93.7(3)
N(2)−Zr−C(27)	113.8(2)	C(6)−N(1)−Zr	143.3(4)
N(1)−Zr−C(20)	95.6(2)	C(13)−N(2)−C(12)	122.2(5)
N(2)−Zr−C(20)	126.4(2)	C(13)−N(2)−Zr	93.1(4)
C(27)−Zr−C(20)	119.6(3)	C(12)−N(2)−Zr	144.5(4)
N(1)−Zr−C(34)	138.9(2)	C(13)−N(3)−Si(1)	117.1(3)
N(2)−Zr−C(34)	84.0(2)	C(13)−N(3)−Si(2)	119.2(4)
C(27)−Zr−C(34)	99.9(3)	Si(1)−N(3)−Si(2)	123.7(3)
C(20)−Zr−C(34)	90.7(2)	C(2)−C(1)−C(6)	111.4(5)
N(1)−Zr−C(26)	107.20(19)	C(1)−C(2)−C(3)	111.7(5)
N(2)−Zr−C(26)	158.43(18)	N(1)−C(13)−N(2)	113.1(5)
C(27)−Zr−C(26)	86.5(2)	N(1)−C(13)−N(3)	123.6(5)
C(20)−Zr−C(26)	33.3(2)	N(2)−C(13)−N(3)	123.3(6)
C(34)−Zr−C(26)	100.2(2)	N(1)−C(13)−Zr	56.4(3)
N(1)−Zr−C(13)	29.86(16)	N(2)−C(13)−Zr	56.9(3)
N(2)−Zr−C(13)	30.00(16)	N(3)−C(13)−Zr	174.7(4)
C(27)−Zr−C(13)	118.2(2)	C(26)−C(20)−Zr	88.7(4)
C(20)−Zr−C(13)	112.0(2)	C(25)−C(26)−C(21)	116.7(7)
C(34)−Zr−C(13)	111.4(2)	C(25)−C(26)−C(20)	121.2(6)
C(26)−Zr−C(13)	134.14(19)	C(21)−C(26)−C(20)	121.3(6)
N(3)−Si(1)−C(14)	108.7(3)	C(25)−C(26)−Zr	94.2(4)
N(3)−Si(1)−C(15)	110.0(3)	C(21)−C(26)−Zr	110.4(4)
N(3)−Si(1)−C(16)	113.0(3)	C(20)−C(26)−Zr	58.1(3)
N(3)−Si(2)−C(19)	109.0(3)	C(33)−C(27)−Zr	116.0(5)
N(3)−Si(2)−C(18)	108.9(3)	C(40)−C(34)−Zr	123.2(4)
N(3)−Si(2)−C(17)	112.3(3)		

The possibility of a significant π interaction between the planar N(SiMe$_3$)$_2$ function of the guanidinate and the bidentate NCN fragment can be ruled out on the basis of the observed dihedral angle of 85.8(3)°.

Conclusions

In summary, guanidinate ligands have proven to be useful in the preparation of a family of bis(guanidinate) and anionic mono(guanidinate) group 4 complexes. A combination of X-ray crystallographic and spectroscopic studies confirm the C_2 symmetric features of the bis(guanidinate) compounds and the structures of the mono(guanidinate) species. From these results, it is clear that little conjugation occurs between the lone pair on the planar NR′$_2$ group and the guanidinate NCN π system. The nearly perpendicular orientation of the NR′$_2$ substituents to the MNCN plane results in a system that appears to exhibit steric features within the plane of the ligand that are similar to those of [RNC(Me)NR]$^-$. The preparation of complex **7** supports the fact that **1**−**6** represent a novel class of potential precursors for soluble organometallic complexes of group 4 free of cyclopentadienyl ligands. The use of the reported complexes to yield catalytically active species is currently under investigation. Along with this effort, our continuing investigations are

(29) Qian, B.; Scanlon, W. J., IV; Smith, M. R., III; Motry, D. H. *Organometallics* **1999**, *18*, 1693.
(30) Scholz, J.; Rehbaum, F.; Theile, K.-H.; Goddard, R.; Betz, P.; Krüger, C. *J. Organomet. Chem.* **1993**, *443*, 93.
(31) Latesky, S. L.; McMullen, A. K.; Niccolai, G. P.; Rothwell, I. P.; Huffman, J. C. *Organometallics* **1985**, *4*, 902.
(32) Jordan, R. F.; Lapointe, R. E.; Baenziger, N.; Hinch, G. D. *Organometallics* **1990**, *9*, 1539.
(33) Jordan, R. F.; Lapointe, R. E.; Bajgur, C. S.; Echols, S. F.; Willett, R. *J. Am. Chem. Soc.* **1987**, *109*, 4111.
(34) Davies, G. R.; Jarvis, J. A. J.; Kilbourn, B. T. *J. Chem. Soc., Chem. Commun.* **1971**, 1511.
(35) Edwards, P. G.; Andersen, R. A.; Zalkin, A. *Organometallics* **1984**, *3*, 293.
(36) Girolami, G. S.; Wilkinson, G.; Thornton-Pett, M.; Hursthouse, M. B. *J. Chem. Soc., Dalton Trans.* **1984**, 2789.
(37) Mintz, E. A.; Moloy, K. G.; Marks, T. J.; Day, V. W. *J. Am. Chem. Soc.* **1982**, *104*, 4692.
(38) Bassi, I. W.; Allegra, G.; Scordamaglia, R.; Chioccola, G. *J. Am. Chem. Soc.* **1971**, *93*, 3787.

oriented at further revealing the steric and electronic features that influence the reactivity of transition metal guanidinate compounds.

Experimental Section

General Considerations. All manipulations were carried out either in a nitrogen-filled drybox or under nitrogen using standard Schlenk-line techniques. $LiN(Si(Me)_3)_2$, $C_6H_{11}NCNC_6H_{11}$, $(CH_3)_2CHNCNCH(CH_3)_2$, $ZrCl_4$, and $HfCl_4$ were used as received from Aldrich Chemical Co. Solvents were distilled under nitrogen from Na/K alloy. $ZrCl_4(THF)_2$ and $HfCl_4(THF)_2$ were prepared by literature procedures. Deuterated benzene was purified by vacuum transfer from potassium metal.

^1H and ^{13}C NMR spectra were run on a Gemini 200 MHz spectrometer with deuterated benzene or pyridine as a solvent and internal standard. All elemental analyses were run on a Perkin-Elmer PE CHN 4000 elemental analysis system.

$Li\{C_6H_{11}NC[N(Si(CH_3)_3)_2]NC_6H_{11}\}$. Addition of a solution of $LiN(Si(Me)_3)_2$ (2.239 g, 13.4 mmol) in 30 mL of diethyl ether to $C_6H_{11}NCNC_6H_{11}$ (2.761 g, 13.4 mmol) in 30 mL of diethyl ether gave a clear pale yellow solution. The reaction mixture was allowed to stir for 4 h. The solvent was removed under vacuum to give a white powder (4.64 g, 93% yield). ^1H NMR (C_6D_6, ppm): 3.38 (br, C_6H_{11}, 2H), 1.95−1.05 (br, C_6H_{11}, 20H), 0.33 (s, CH_3, 18H). ^{13}C NMR (C_6D_6, ppm): 163.90 (s, $N_3\boldsymbol{C}$), 54.29, 38.70, 26.62, 26.13 (4s, $\boldsymbol{C}_6H_{11}$), 2.63 (s, $\boldsymbol{C}H_3$)

$Li\{(CH_3)_2CHNC[N(Si(CH_3)_3)_2]NCH(CH_3)_2\}$. Addition of a solution of $LiN(Si(CH_3)_3)_2$ (2.850 g, 17.0 mmol) in 30 mL of diethyl ether to $(CH_3)_2CHNCNCH(CH_3)_2$ (2.150 g, 17.0 mmol) in 20 mL of diethyl ether gave a clear pale yellow solution. The mixture was allowed to stir for 4 h. The solvent was removed under vacuum to give a very light peach-colored solid (4.34 g, 87% yield). ^1H NMR (C_6D_6, ppm): 3.72 (sept, CH, 2H), 1.12 (d, CH_3, 12H), 0.31 (s, CH_3, 18H). ^{13}C NMR (C_6D_6, ppm): 163.95 (s, $N_3\boldsymbol{C}$), 45.70, 27.71 (2s, $\boldsymbol{C}H(\boldsymbol{C}H_3)_2$), 2.56 (s, $\boldsymbol{C}H_3$).

$Zr[(CH_3)_2CHNC(N(Si(CH_3)_3)_2)NCH(CH_3)_2]_2Cl_2$ (1). A reaction flask was charged with $ZrCl_4(THF)_2$ (0.568 g, 1.51 mmol), 50 mL of diethyl ether, and a stir bar. To this was added $Li[(CH_3)_2CHNC(Si(CH_3)_3)_2NCH(CH_3)_2]$ (0.906 g, 3.09 mmol). After the reaction mixture was allowed to stir for 16 h, the mixture was filtered and the solvent was evaporated from the clear yellow filtrate under vacuum to give a pale yellow powder (0.464 g, 42%). Colorless crystals were obtained from toluene at −34 °C. ^1H NMR (C_6D_6, ppm): 3.93 (sept, CH, 4H), 1.48 (d, CH_3, 24H), 0.25 (s, CH_3, 36H). ^{13}C NMR (C_6D_6, ppm): 175.23 (s, $N_3\boldsymbol{C}$), 47.33 (s, $\boldsymbol{C}H(CH_3)_2$), 25.47 (s, $CH(\boldsymbol{C}H_3)_2$), 2.90 (s, $Si\boldsymbol{C}H_3$). Anal. Calcd for $ZrCl_2Si_4N_6C_{26}H_{64}$: C, 42.47; H, 8.77; N, 11.43. Found: C, 42.94; H, 8.90; N, 10.86.

$Hf[(CH_3)_2CHNC(N(Si(CH_3)_3)_2)NCH(CH_3)_2]_2Cl_2$ (2). An experimental procedure similar to that for **1** using $HfCl_4(THF)_2$ (1.129 g, 2.43 mmol) and $Li[(CH_3)_2CHNC(Si(CH_3)_3)_2NCH(CH_3)_2]$ (1.463 g, 4.98 mmol) in diethyl ether gave an off-white powder (1.399 g, 70% yield). Colorless crystals were obtained from toluene at −34 °C. ^1H NMR (C_6D_6, ppm): 4.11 (sept, $CH(CH_3)_2$, 4H), 1.48 (d, $CH(CH_3)_2$, 24H), 0.25 (s, CH_3, 36H). ^{13}C NMR (C_6D_6, ppm): 174.69 (s, $N_3\boldsymbol{C}$), 47.02 (s, $\boldsymbol{C}H(CH_3)_2$), 25.48 (s, $CH(\boldsymbol{C}H_3)_2$), 2.93 (s, $Si\boldsymbol{C}H_3$). Anal. Calcd for $HfCl_2Si_4N_6C_{26}H_{64}$: C, 37.96; H, 7.84; N, 10.22. Found: C, 37.60; H, 7.80; N, 9.77.

$Zr[C_6H_{11}NC(Si(CH_3)_3)_2NC_6H_{11}]_2Cl_2$ (3). An experimental procedure similar to that for **1** using $ZrCl_4(THF)_2$ (0.421 g, 1.1 mmol) and $Li[C_6H_{11}NC(Si(CH_3)_3)_2NC_6H_{11}]$ (0.855 g, 2.3 mmol) gave a very light yellow solid (0.72 g, 73% yield). Colorless crystals were obtained from toluene at −34 °C. ^1H NMR (C_6D_6, ppm): 3.50 (br, C_6H_{11}, 4H), 1.0−2.2 (br, C_6H_{11}, 40H), 0.3 (s, CH_3, 36H). ^{13}C NMR (C_6D_6, ppm): 175.17 (s, $N_3\boldsymbol{C}$), 56.08, 35.36, 35.17, 26.34 (4s, $\boldsymbol{C}_6H_{11}$), 3.12 (s, $Si\boldsymbol{C}H_3$).

$Hf[C_6H_{11}NC(Si(CH_3)_3)_2NC_6H_{11}]_2Cl_2$ (4). An experimental procedure similar to that for **1** using $HfCl_4(THF)_2$ (1.418 g, 3.1 mmol) and $Li[C_6H_{11}NC(Si(CH_3)_3)_2NC_6H_{11}]$ (2.338 g, 6.3 mmol) gave a white powder (2.54 g, 83% yield). Colorless crystals were obtained from toluene at −34 °C. ^1H NMR (C_6D_6, ppm): 3.68 (br, C_6H_{11}, 4H), 1.90−1.20 (br, C_6H_{11}, 40H), 0.32 (s, CH_3, 36H). ^{13}C NMR (C_6D_6, ppm): 174.61 (s, $N_3\boldsymbol{C}$), 55.66, 35.03, 26.26, 25.61 (4s, $\boldsymbol{C}_6H_{11}$), 3.17 (s, $Si\boldsymbol{C}H_3$). Anal. Calcd for $C_{38}H_{80}N_6Si_4HfCl_2$: C, 46.44; H, 8.20; N, 8.55. Found: C, 46.18; H, 8.31; N, 8.36.

$Zr\{[C_6H_{11}NC(Si(CH_3)_3)_2NC_6H_{11}]Cl_4\}Li(THF)_2[O(CH_2CH_3)_2]$ (5). A reaction flask was charged with $ZrCl_4(THF)_2$ (1.333 g, 3.5 mmol), 50 mL of diethyl ether, and a stir bar. To this was added $Li[C_6H_{11}NC(Si(CH_3)_3)_2NC_6H_{11}]$ (1.320 g, 3.5 mmol). After 20 h of stirring, the reaction mixture was filtered through Celite to give a clear pale lemon yellow filtrate. The solvent was then removed under vacuum to give a very light green powder (1.96 g, 68% yield). Pale-yellow crystals were obtained from diethyl ether at −34 °C. ^1H NMR (py-d_5, ppm): 3.75 (br m, C_6H_{11}, 2H), 3.60 (m, THF, 8H), 3.31(q, Et_2O, 4H), 2.68−1.26 (br, C_6H_{11}, 20H), 1.61 (m, THF, 8H), 1.12 (t, Et_2O, 6H), 0.43 (s, CH_3, 18H). ^{13}C NMR (py-d_5, ppm): 171.93 (s, $N_3\boldsymbol{C}$), 67.77, 25.41 (2s, THF), 65.72, 15.46 (2s, diethyl ether), 55.76, 34.89, 25.99, 25.77 (4s, $\boldsymbol{C}_6H_{11}$), 2.56 (s, $\boldsymbol{C}H_3$).

$Hf\{[C_6H_{11}NC(N(Si(CH_3)_3)_2)NC_6H_{11}]Cl_4\}\{Li(THF)_3\}$ (6). An experimental procedure similar to that for **5** using $HfCl_4(THF)_2$ (0.713 g, 1.5 mmol) and $Li[C_6H_{11}NC(Si(CH_3)_3)_2NC_6H_{11}]$ (0.573 g, 1.5 mmol) gave a colorless filtrate. The solvent was then removed under vacuum to give a white powder (0.908 g, 66% yield). Colorless crystals were obtained from diethyl ether at −34 °C. ^1H NMR (py-d_5, ppm): 3.75 (br, C_6H_{11}, 2H), 3.62 (m, THF, 12H), 2.68−1.25 (br, C_6H_{11}, 20H), 1.59 (m, THF, 12H), 0.43 (s, CH_3, 18H). ^{13}C NMR (py-d_5, ppm): 170.29 (s, $N_3\boldsymbol{C}$), 67.81, 25.79 (2s, THF), 55.43, 35.05, 26.43, 26.06 (4s, $\boldsymbol{C}_6H_{11}$), 2.64 (s, $\boldsymbol{C}H_3$).

$[C_6H_{11}NC(Si(CH_3)_3)_2NC_6H_{11}]Zr(CH_2C_6H_5)_3$ (7). In a reaction flask, compound **5** (1.000 g, 1.21 mmol) was dissolved in 10 mL of toluene. To the stirring solution was added dropwise $C_6H_5CH_2MgCl$ (4.5 mL, 1.0 M in diethyl ether), and the reaction mixture was allowed to stir for 2 h. Removal of solvent followed by extraction of the resultant solid with 10 mL of toluene, filtration, concentration, and cooling to −34 °C gave orange crystals (0.64 g, 72%). ^1H NMR(C_6D_6, ppm): 7.22−6.91 (mult, C_6H_5, 15H), 3.50 (br, CH, 2H), 2.50 (s, CH_2, 6H), 1.75−0.88 (br, C_6H_{11}, 10H), 0.18 (s, CH_3, 9H). ^{13}C NMR (C_6D_6, ppm): 174.19 (s, $N_3\boldsymbol{C}$), 144.75 (s, $\boldsymbol{C}_6H_5$), 129.43, 128.22, 122.83 (3s, C_6H_5), 77.36 (s, $\boldsymbol{C}H_2$), 56.38 (s, $\boldsymbol{C}H$), 35.07, 26.45, 25.68 (3s, $\boldsymbol{C}_6H_{11}$), 2.36 (s, $\boldsymbol{C}H_3$).

Acknowledgment. This work was supported by the Natural Sciences and Engineering Research Council of Canada.

Supporting Information Available: Listings of crystal data and structure refinement details, atomic coordinates, bond distances, bond angles, and thermal parameters for **3**, **4**, and **6** and X-ray crystallographic files in CIF format for the structure determinations of **1**, **5**, and **7** and in SHELXT.TEX format for the structure determinations of **3**, **4**, and **6**. This material is available free of charge via the Internet at http://pubs.acs.org.

IC990668I